

## Effect of Kerr nonlinearity on defect lasing modes in weakly disordered photonic crystals

B. Liu, A. Yamilov, and H. Cao<sup>a)</sup>

Department of Physics and Astronomy, Northwestern University, 2145 Sheridan Road, Evanston, Illinois 60208-3112

(Received 3 December 2002; accepted 16 June 2003)

We studied the effect of Kerr nonlinearity on lasing in defect modes of weakly disordered photonic crystals. Our time-independent calculation based on self-consistent nonlinear transfer matrix method shows that Kerr nonlinearity modifies both frequencies and quality factors of defect modes. We also used a time-dependent algorithm to investigate the dynamic nonlinear effect. Under continuous pumping, the spatial sizes and intensities of defect lasing modes are changed by Kerr nonlinearity. Such changes are sensitive to the nonlinear response time. © 2003 American Institute of Physics. [DOI: 10.1063/1.1598286]

Kerr nonlinearity results in a dependence of refractive index on light intensity:  $n = n_0 + n_2|E|^2$ , where  $n_0$  is the linear refractive index,  $n_2$  is the nonlinear Kerr coefficient, and  $|E|$  is the electric field amplitude. When a light beam travels in a *homogeneous* Kerr medium, positive nonlinearity ( $n_2 > 0$ ) always leads to self-focusing, while negative nonlinearity ( $n_2 < 0$ ) self-defocusing. However, in an *inhomogeneous* medium, light transport behavior is not simply determined by the sign of Kerr nonlinearity. The interference effect of scattered waves dominates light transport in a linear inhomogeneous medium. For example, in a periodic structure (photonic crystal, PC), constructive and destructive interferences result in pass bands and stop bands for light propagation.<sup>1</sup> In a weakly disordered PC, defect modes are formed near the band edges.<sup>2</sup> Such modes are spatially localized and have high quality factors ( $Q$ ). In the presence of optical gain, they serve as lasing modes.<sup>3</sup> The nonlinear effect on defect lasing modes is significant owing to high laser intensity and resonance enhancement. Specifically, the nonlinearity at the lasing frequency, which is in resonance with a transition of the gain material, is resonantly enhanced.

Over the past few years, there have been extensive studies on nonlinear PCs and their applications to switches, limiters, optical diodes, and transistors in integrated photonic circuits.<sup>4-7</sup> However, these studies are focused on passive systems. The nonlinear effect in active PCs has not been well understood. In this letter, we modeled the effect of Kerr nonlinearity on defect lasing modes in weakly disordered PCs. We took two approaches: (i) time-independent calculation based on self-consistent nonlinear transfer matrix method and (ii) time-dependent simulation with the finite-difference time-domain (FDTD) method. With the first approach, we investigated how Kerr nonlinearity changes the frequency and quality factor of a defect mode. The second method reveals the dynamic effect of Kerr nonlinearity on the spatial size and intensity of a defect lasing mode. Physical interpretation of these results are presented. *How fast the nonlinear response is* turns out to be essential to the dynamic nonlinear effect in an active nonlinear system.

The model system in our study is a weakly disordered one-dimensional PC. It consists of binary layers made of dielectric materials with dielectric constants  $\epsilon_1 = \epsilon_0$  and  $\epsilon_2 = 9\epsilon_0$ , respectively. The thickness of the first layer, which simulates the gain medium, is  $a = a_0(1 + w_a\alpha)$ , where  $a_0 = 400$  nm,  $w_a$  represents the degree of disorder, and  $\alpha$  is a random value in the range  $[-0.5, 0.5]$ . The thickness of the second layer, which simulates the nonlinear medium, is  $b = b_0(1 + w_b\beta)$ , where  $b_0 = 100$  nm,  $w_b$  represents the degree of disorder, and  $\beta$  is a random value in the range  $[-0.5, 0.5]$ .

We first investigated how Kerr nonlinearity modifies the defect modes of a passive system in the time-independent calculation. We used a self-consistent nonlinear transfer matrix method for this study.<sup>8,9</sup> This method works only in the perturbative regime; that is, the nonlinear refractive index change  $|\Delta n| = |n_2| \cdot |E|^2 \ll n_0$ . In Fig. 1 we considered two defect modes in a weakly disordered pc ( $W_a = W_b = 0.2$ ) with 50 layers. One mode ( $\lambda \sim 6988$  Å) is on the short wavelength edge of a band gap, the other ( $\lambda \sim 8632$  Å) is on the long wavelength edge of the same gap. Figure 1 shows the transmission peaks of these two defect modes. The values of  $n_2$  are chosen such that the maximum change of refractive index  $|\Delta n|_{\max} = |n_2| \cdot |E_{\max}|^2 < 1 \times 10^{-2}$ . Positive Kerr nonlinearity ( $n_2 > 0$ ) always shifts the defect modes toward longer wavelength, while the negative nonlinearity ( $n_2 < 0$ ) to shorter wavelength. In Fig. 1, the wavelength shift is  $\sim 4$  Å, and it is nearly symmetric (although not exactly) for positive and negative  $n_2$ . From the center wavelength  $\lambda_0$  and linewidth  $\Delta\lambda$ , we calculated the defect mode's quality factor  $Q = \lambda_0/\Delta\lambda$ . The change of  $Q$  depends not simply on the nonlinearity, but on the position of the defect modes with respect to the band gaps. For the defect mode at 6988 Å [Fig. 1(a)], positive Kerr nonlinearity increases its  $Q$ . On the contrary, for the defect mode at 8632 Å [Fig. 1(b)], positive Kerr nonlinearity decreases its  $Q$ . We repeated this calculation for many defect modes in different structures. We found the general behavior: when the Kerr nonlinearity moves a defect mode closer to the center of a band gap,  $Q$  increases; otherwise  $Q$  decreases. This can be understood in terms of the change of localization length  $\xi$ . In the presence of weak dis-

<sup>a)</sup>Electronic mail: h-cao@northwestern.edu

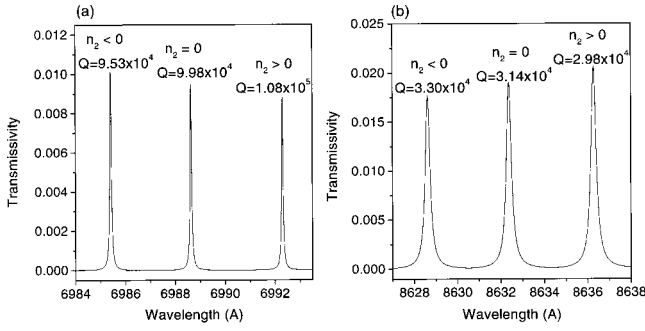


FIG. 1. Transmission peaks of the two defect modes (specified in Fig. 1) in the presence of Kerr nonlinearity. The quality factors are written next to the peaks. (a)  $n_2 = 5.0 \times 10^{-7} \text{ m}^2/\text{V}^2$ ,  $|\Delta n|_{\text{max}} = |n_2| \cdot |E_{\text{max}}|^2 = 7.45 \times 10^{-3}$ ,  $n_2 = -5.0 \times 10^{-7} \text{ m}^2/\text{V}^2$ ,  $|\Delta n|_{\text{max}} = 6.55 \times 10^{-3}$ . (b)  $n_2 = 1.0 \times 10^{-3} \text{ m}^2/\text{V}^2$ ,  $|\Delta n|_{\text{max}} = 8.76 \times 10^{-3}$ ,  $n_2 = -1.0 \times 10^{-3} \text{ m}^2/\text{V}^2$ ,  $|\Delta n|_{\text{max}} = 8.48 \times 10^{-3}$ .

order, the defect modes are located near the band edges where  $d\xi/d\lambda \neq 0$ . The closer to the band gap center, the shorter  $\xi$ . For a defect mode on the shorter wavelength side of a stop band where  $d\xi/d\lambda < 0$ , positive Kerr nonlinearity redshifts its wavelength toward the band gap center. The decrease of the localization length  $\xi$  leads to better confinement of defect modes, thus higher  $Q$ . In contrast, for a defect mode on the longer wavelength side of a stop band where  $d\xi/d\lambda > 0$ , positive Kerr nonlinearity redshifts its wavelength away from the stop-band center. The increase of  $\xi$  results in worse optical confinement and lower  $Q$ . More quantitatively, the quality factor of a defect mode can be estimated as  $Q \propto \exp(L/\xi)$ , where  $L$  is the system length.<sup>10</sup> The nonlinear shift of mode wavelength causes a change of  $\xi$ , which affects the value of  $Q$ . The change of  $Q$  can be estimated as  $\Delta Q/Q \propto -(L/\xi^2) \cdot \Delta\xi \propto -(L/\xi) \cdot [(d\xi/d\lambda) \cdot (\Delta\lambda/\lambda)]$ . The first two factors in this expression can be large; in our case they are on the order of 10. This explains why, in our numerical calculation, the relative change of  $Q$  is about 2 orders of magnitude larger than the relative change of mode wavelength. Moreover, the sign of  $d\xi/d\lambda$ , opposite on the two sides of a band gap, determines the sign of  $\Delta Q$ . However, in the presence of strong disorder, the defect modes move to the stop band centers where  $d\xi/d\lambda \approx 0$ . Their quality factors do not exhibit systematic changes.

The limitation of the self-consistent nonlinear transfer matrix method is that it works only for *passive* media at the *steady* state. To study the dynamic nonlinear effect in an active medium, we switched to a time-dependent algorithm. We solved the time-dependent Maxwell equations with the FDTD method.<sup>11</sup> In the layers of gain medium we solved the rate equations for 4-level atoms.<sup>12</sup> In the dielectric layers with Kerr nonlinearity, we introduced the nonlinear polarization density<sup>13,14</sup>  $P_{\text{NL}}(x,t) = \epsilon_0 \chi^{(3)} E(x,t) \int_{-\infty}^t g(t-\tau) |E(x,\tau)|^2 d\tau$ , where  $\chi^{(3)}$  is the third-order nonlinear susceptibility. The casual response function  $g(t-\tau) = (1/\tau_0) \exp[-(t-\tau)/\tau_0]$  for  $t \geq \tau$ , and  $g(t-\tau) = 0$  for  $t < \tau$ .  $\tau_0$  is the nonlinear response time. To incorporate the nonlinearity with finite-time response into the FDTD algorithm, we introduced a new function  $G(x,t) \equiv \int_{-\infty}^t g(t-\tau) |E(x,\tau)|^2 d\tau = (1/\tau_0) \int_0^t e^{-(t-\tau)/\tau_0} |E(x,\tau)|^2 d\tau$ . The differential equation for  $G(x,t)$  can be derived as

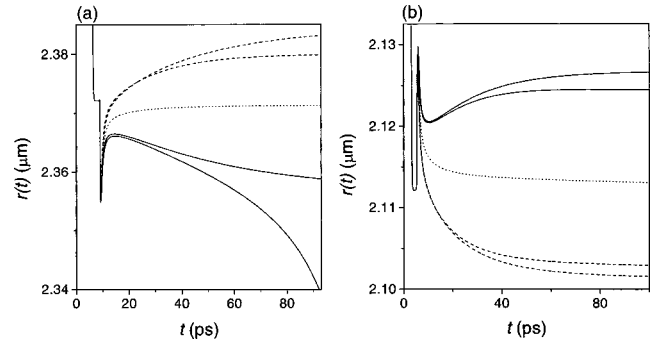


FIG. 2. Spatial size  $r(t)$  of the two defect lasing modes at the pumping rate of  $5.0 \times 10^7 \text{ s}^{-1}$ . (a) For the defect mode at 6988 Å. From top to bottom:  $\chi^{(3)} = -1.0 \times 10^{-17} \text{ m}^2/\text{V}^2$  and  $\tau_0 = 500T$ ;  $\chi^{(3)} = -1.0 \times 10^{-17} \text{ m}^2/\text{V}^2$  and  $\tau_0 = 5T$ ;  $\chi^{(3)} = 0$ ;  $\chi^{(3)} = 1.0 \times 10^{-17} \text{ m}^2/\text{V}^2$  and  $\tau_0 = 500T$ ;  $\chi^{(3)} = -1.0 \times 10^{-17} \text{ m}^2/\text{V}^2$  and  $\tau_0 = 5T$ . (b) For the mode at 8632 Å. From top to bottom:  $\chi^{(3)} = 8.0 \times 10^{-17} \text{ m}^2/\text{V}^2$  and  $\tau_0 = 5T$ ;  $\chi^{(3)} = 8.0 \times 10^{-17} \text{ m}^2/\text{V}^2$  and  $\tau_0 = 500T$ ;  $\chi^{(3)} = 0$ ;  $\chi^{(3)} = -8.0 \times 10^{-17} \text{ m}^2/\text{V}^2$  and  $\tau_0 = 5T$ ;  $\chi^{(3)} = -8.0 \times 10^{-17} \text{ m}^2/\text{V}^2$  and  $\tau_0 = 500T$ .

$$\frac{dG(x,t)}{dt} = -\frac{G(x,t)}{\tau_0} + \frac{|E(x,t)|^2}{\tau_0}. \quad (1)$$

$E$  is related to  $D$  by accounting for both linear polarization  $P_L$  and nonlinear polarization  $P_{\text{NL}}$ :  $E(x,t) = [D(x,t) - P_L(x,t) - P_{\text{NL}}(x,t)]/\epsilon_0 \epsilon_\infty$ . Because  $P_L = \epsilon_0 \chi^{(1)} E$  and  $P_{\text{NL}} = \epsilon_0 \chi^{(3)} E G$ , the effective dielectric constant is  $\epsilon(x,t) = \epsilon_\infty + \chi^{(1)} + \chi^{(3)} G(x,t)$ , where  $\chi^{(1)}$  is the linear susceptibility. When light frequency is far from any resonant frequencies,  $\tau_0$  approaches 0, Kerr nonlinearity becomes instantaneous,  $g(t-\tau) = \delta(t-\tau)$ , and  $G(x,t) = |E(x,t)|^2$ . The nonlinear dielectric constant  $\epsilon = \epsilon_L + \chi^{(3)} |E|^2$ , where  $\epsilon_L = \epsilon_\infty + \chi^{(1)}$  is the linear dielectric constant. Hence, the nonlinear refractive index  $n = n_0 + n_2 |E|^2$ , where  $n_0 = \sqrt{\epsilon_L}$ ,  $n_2 = \chi^{(3)}/2n_0$ .

In our time-dependent calculation, we first turned off Kerr nonlinearity by setting  $\chi^{(3)} = 0$ . Initially, all the atoms are in the ground state. The external pumping is switched on at  $t=0$ , and kept constant. Its value is chosen so that only one defect mode lases. The lasing frequency is nearly identical to the frequency of the defect mode in the passive system. Next, we included Kerr nonlinearity ( $\chi^{(3)} \neq 0$ ). A significant frequency shift of the defect lasing mode is observed. Positive nonlinearity ( $\chi^{(3)} > 0$ ) leads to redshift, while negative nonlinearity ( $\chi^{(3)} < 0$ ) to blueshift. This result is consistent with that of the nonlinear transfer matrix method.

The spatial size of a defect lasing mode is also changed by Kerr nonlinearity. When only one mode lases, the size of the lasing mode can be characterized by the inverse partition ratio  $r(t) = (\int |E(x,t)|^2 dx)^2 / (\int |E(x,t)|^4 dx)$ . Figure 2 plots  $r(t)$  of two defect lasing modes (the same ones as in Fig. 1). The values of  $\chi^{(3)}$  are chosen so that the wavelength shifts of these two modes are  $\sim 4 \text{ \AA}$ , close to their shifts in the nonlinear transfer matrix calculation. For  $\chi^{(3)} > 0$ , the defect mode at 6988 Å increases in size, while the defect mode at 8632 Å shrinks. The size  $r$  of a spatially localized defect mode is on the order of the localization length  $\xi$ . Therefore, the relative change of the size can be estimated as  $\Delta r/r \propto [(d\xi/d\lambda) \cdot (\Delta\lambda/\lambda)]$ . The sign of  $d\xi/d\lambda$  is different on the opposite sides of the band gap, which explains the

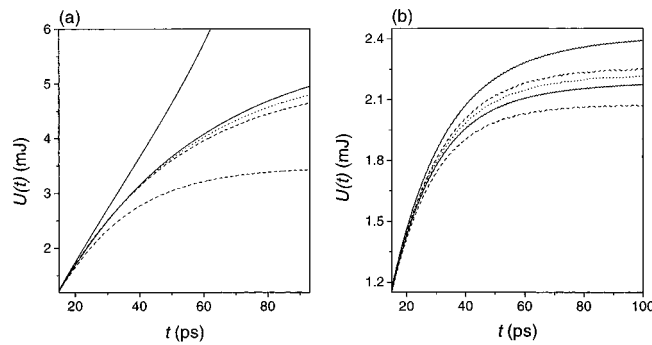


FIG. 3. Total laser emission energy  $U(t)$  of the two defect lasing modes at the pumping rate of  $5.0 \times 10^7 \text{ s}^{-1}$ . (a) For the defect mode at  $6988 \text{ \AA}$ . From top to bottom:  $\chi^{(3)} = 1.0 \times 10^{-17} \text{ m}^2/\text{V}^2$  and  $\tau_0 = 5T$ ;  $\chi^{(3)} = 1.0 \times 10^{-17} \text{ m}^2/\text{V}^2$  and  $\tau_0 = 500T$ ;  $\chi^{(3)} = 0$ ;  $\chi^{(3)} = -1.0 \times 10^{-17} \text{ m}^2/\text{V}^2$  and  $\tau_0 = 500T$ ;  $\chi^{(3)} = -1.0 \times 10^{-17} \text{ m}^2/\text{V}^2$  and  $\tau_0 = 5T$ . (b) For the mode at  $8632 \text{ \AA}$ . From top to bottom:  $\chi^{(3)} = 8.0 \times 10^{-17} \text{ m}^2/\text{V}^2$  and  $\tau_0 = 5T$ ;  $\chi^{(3)} = -8.0 \times 10^{-17} \text{ m}^2/\text{V}^2$  and  $\tau_0 = 500T$ ;  $\chi^{(3)} = 0$ ;  $\chi^{(3)} = 8.0 \times 10^{-17} \text{ m}^2/\text{V}^2$  and  $\tau_0 = 500T$ ;  $\chi^{(3)} = -8.0 \times 10^{-17} \text{ m}^2/\text{V}^2$  and  $\tau_0 = 5T$ .

sign of mode-size change. The size change of a defect lasing mode is consistent with the change of its  $Q$  predicted by the nonlinear transfer matrix method. With an increase in the size of a defect mode, its loss caused by light leakage through the boundary increases; thus, its  $Q$  decreases.

As shown in Fig. 2, the final (steady-state) size of defect lasing modes also depends on the nonlinear response time  $\tau_0$ . Nevertheless,  $\tau_0$  only affects the magnitude of  $\Delta r$ , it does not flip the sign of  $\Delta r$ . However, it is not so for laser intensity. We calculated the total laser emission energy  $U(t) = (1/2) \int \epsilon_0 \epsilon |E(x,t)|^2 dx$  under constant pumping. As shown in Fig. 3, when  $\tau_0 = 500T$  ( $T$  is the optical period), the intensity change of a defect lasing mode is consistent with its size change. Namely, when the Kerr nonlinearity reduces the size of a defect mode, the increase of its  $Q$  leads to stronger laser emission. From the mode size  $r$ , we estimated the time it takes light to travel across the defect mode,  $\tau_c \sim r/c \sim 5T$ . When  $\tau_0$  is shortened to  $5T$ , the phenomenon is very different. Positive nonlinearity always results in stronger laser emission, while negative nonlinearity weak laser emission regardless the size change.

From the calculation of many defect lasing modes, we conclude that the effect of Kerr nonlinearity on laser intensity depends on the relative magnitude of  $\tau_0$  versus  $\tau_c$ . When  $\tau_0$  is shorter than  $\tau_c$ , the change of laser intensity depends only on the sign of Kerr nonlinearity; that is, positive nonlinearity always extract more laser emission from the system at the same pumping rate. During the buildup of lasing oscillation, the phase of light field reflected by (or transmitted through) each nonlinear layer changes quickly owing to rapid change of its refractive index with intensity. The lack of constant phase relation among multiple reflected waves undermines the interference effect. Hence, the single reflection dominates the feedback for lasing. For  $\chi^{(3)} > 0$ , the refractive index contrast of the binary layers increases with

the laser intensity. Reflectivity at the layer interface becomes larger, giving stronger feedback for lasing. Thus laser emission is enhanced. When  $\tau_0$  is longer than  $\tau_c$ , the nonlinear change of refractive index is slow enough that the interference of multiple reflected waves still dominates the feedback for lasing. Thus, the intensity change of a defect lasing mode depends on the change of its size and  $Q$ .

Note that the difference between our study and that on nonlinear localized modes (also called intrinsic localized modes or discrete breathers)<sup>15</sup> is that our localized modes are formed by defects instead of nonlinearity. The nonlinearity merely modifies the defect modes *perturbatively*. Our model works only when the nonlinear change of refractive index  $\Delta n \ll n_0$ . However, for positive and fast nonlinearity, the rapid nonlinear feedback to lasing may lead the system out of the perturbative regime, as shown by the lower solid trace in Fig. 2(a) and the top solid curve in Fig. 3(a). When  $\Delta n \sim n_0$ , the higher order nonlinearity must be taken into account, and our calculation result is no longer accurate. Nevertheless, in many practical systems Kerr nonlinearity is weak; for example, the fiber distributed-feedback laser.<sup>16</sup> Our results illustrate that dynamic nonlinear effect is significant not only to the transient process but also to the final lasing state under constant pumping. Therefore, even in the presence of weak nonlinearity, time-dependent modeling is essential to correctly predict the lasing behavior. Our time-dependent FDTD calculation reveals that the speed of nonlinear response is an important factor in the Kerr effect on lasing.

The authors acknowledge Prof. A. Taflove, Dr. A. L. Burin, and S.-H. Chang for stimulating discussions. This work is supported partially by the National Science Foundation under Grant No. DMR-0093949 and the David and Lucille Packard Foundation.

<sup>1</sup>J. D. Joannopoulos, R. D. Meade, and J. N. Winn, *Photonic Crystals: Molding the Flow of Light* (Princeton University Press, Princeton, 1995).

<sup>2</sup>S. John, *Phys. Rev. Lett.* **58**, 2486 (1987).

<sup>3</sup>A. Yamilov and H. Cao, cond-mat/0209680.

<sup>4</sup>M. Scalora, J. P. Dowling, C. M. Bowden, and M. J. Bloemer, *Phys. Rev. Lett.* **73**, 1368 (1994).

<sup>5</sup>V. Berger, *Phys. Rev. Lett.* **81**, 4136 (1998).

<sup>6</sup>S. F. Mingaleev and Yu. S. Kivshar, *J. Opt. Soc. Am. B* **19**, 2241 (2002).

<sup>7</sup>M. Soljacic, S. G. Johnson, S. Fan, M. Ibanescu, E. Ippen, and J. D. Joannopoulos, *J. Opt. Soc. Am. B* **19**, 2052 (2002).

<sup>8</sup>J. He and M. Cada, *Appl. Phys. Lett.* **61**, 2150 (1992).

<sup>9</sup>V. Lousse and J.-P. Vigneron, *Synth. Met.* **116**, 461 (2001).

<sup>10</sup>M. Ya. Azbel, *Solid State Commun.* **45**, 527 (1983); L. I. Deych, A. Yamilov, and A. A. Lisyansky, *Phys. Rev. B* **64**, 075321 (2001).

<sup>11</sup>A. Taflove and S. C. Hagness, *Computational Electrodynamics: the Finite-Difference Time-Domain Method* (Artech House, Boston, 2000).

<sup>12</sup>A. S. Nagra and R. A. York, *IEEE Trans. Antennas Propag.* **46**, 334 (1998).

<sup>13</sup>R. W. Ziolkowski and J. B. Judkins, *J. Opt. Soc. Am. B* **10**, 186 (1993).

<sup>14</sup>R. M. Joseph and A. Taflove, *IEEE Trans. Antennas Propag.* **45**, 364 (1997).

<sup>15</sup>S. F. Mingaleev and Yu. S. Kivshar, *Phys. Rev. Lett.* **86**, 5474 (2001).

<sup>16</sup>Y. H. Lian and H. G. Winful, *Opt. Lett.* **21**, 471 (1996).